Journal of Solid State Chemistry **144,** 25–29 (1999)
Article ID jssc.1998.8089, available online at http://www.idealibrary.com on IDEAL®

Characterization of Various Magnesium Oxides by XRD and ^{1}H MAS NMR Spectroscopy

María Angeles Aramendía, José Antonio Benítez, Victoriano Borau, César Jiménez, José María Marinas, José Rafael Ruiz, and Francisco Urbano

Departamento de Química Orgánica, Universidad de Córdoba, Avenida San Alberto Magno s/n, E-14004 Córdoba, Spain

Received May 29, 1998; in revised form October 23, 1998; accepted October 27, 1998

A magnesium oxide obtained by thermal decomposition of commercially available magnesium hydroxide was refluxed in water and acetone in order to improve its chemical and textural properties with the purpose of using it as a support for metals in heterogeneous catalysts. X-ray diffraction, CO_2 chemisorption, and ^{1}H magic-angle spinning nuclear magnetic resonance were used to identify crystal phases, the number of basic sites, and the nature of OH groups in the oxide, respectively.

Key Words: **magnesium oxide; ^{1}H MAS NMR; X-ray diffraction; CO_2 chemisorption.**

INTRODUCTION

Molecular conversions on solid surfaces are the result of interactions of the molecules with surface active sites either naturally occurring on catalyst surfaces (e.g., surface OH groups, atoms or defects) or obtained by special preparation techniques (e.g., supported acids and bases, metals, metal oxides, organometallic compounds). Specifically, magnesium oxide exhibits strong basicity by virtue of the presence of surface O^{2-} ions that capture protons readily. It also exhibits weak Lewis basicity that is ascribed to Mg^{2+} ions.

Because of its low specific surface area, magnesium oxide has seldom been used as a support in metal catalysts. In recent years, our research group has conducted extensive work aimed at obtaining magnesium oxides with high specific surface areas (1–3), which are suitable for use as catalysts or catalyst supports. Hydration of the solid and its subsequent calcination at 673 K reportedly increases its surface area (4), Magnesium oxide is also interesting because it has the ability to stabilize metals in unusual oxidation states, and avoids sintering and evaporation of the metal atoms (5, 6). There is abundant evidence that metal reactivity is affected by the presence of MgO as support (7–11).

In recent years, high-resolution solid-state nuclear magnetic resonance (NMR) spectroscopy has grown dramatically in use as a complement to electron diffraction techniques for the characterization of crystalline solids. Solid-state NMR spectroscopy has also become a useful tool for examining amorphous solids, which are not detected by the X-ray diffraction technique, as it allows one to characterize the local environment of the atom or atoms that seemingly constitute active sites. Characterization of the chemical nature of surface active sites and of their properties are two major goals in catalysis research that have so far been pursued by using a variety of physical techniques including IR, visible, UV, and Raman spectroscopies, and ESR, ESCA, EXAFS, and X-ray diffraction (XRD), among others. Specifically, ^{1}H MAS NMR spectroscopy was recently used for the structural elucidation of alumina (12–14), titanium oxide (15), vanadium oxide–aluminum orthophosphate systems (16), sepiolites (17), Mg/Ga double-layered hydroxides (18), magnesium pyrophosphate (19), and zeolites (20–22).

In this work, a magnesium oxide from commercially available magnesium hydroxide was synthesized. The oxide was treated in two different ways with the purpose of improving its chemical textural properties, which were determined by various techniques. Thus, X-ray diffraction was used to assess the degree of crystallinity and ^{1}H magic-angle spinning (MAS) NMR to identify OH surface groups. The treatments were intended to improve the chemical textural properties of the different oxides with a view to their use as supports for metal systems, where deposition by impregnation entails using a solvent such as acetone or distilled water for the metal salt precursor.

EXPERIMENTAL

Materials

Magnesium oxide was obtained by calcination of commercially available $Mg(OH)_2$ (Merck ref. 105.870) at 873 K in air for 2 h. The resulting solid was called MgO_s and was used to obtain various other magnesium oxides by following two different procedures, namely, (a) refluxing in distilled water for 6 h and subsequent calcination at 873 K in air for

0022-4596/99 $30.00

2 h, which yielded solid MgO_w; and (b) refluxing in acetone for 6 h and calcination at 873 K in air for 2 h, which yielded solid MgO_{AC}. Commercially available MgO (Aldrich ref. 24,338-8), labeled MgO_C, was used for comparison.

Textural Properties

The textural properties of the solids (specific surface area, pore volume, and mean pore radius) were determined from nitrogen adsorption–desorption isotherms obtained at liquid nitrogen temperature on a Micromeritics ASAP-2010 instrument. Surface areas were calculated by the Brunauer–Emmett–Teller (BET) method (23), while pore distributions were determined by the Barrett–Joynet–Halenda (BJH) method (24) (adsorption branch, cylindrical pores open on one side only, and adsorbed layer thickness as calculated by the Halsey method). All samples were degassed at 423 K at a pressure below 3 μm of Hg prior to analysis.

TPD Measurements

Recently, our research group developed a procedure for determining basic sites in active solids (25) that is a combination of thermal programmed desorption (TPD) and mass spectrometry (MS). Amounts of chemisorbed CO_2 were determined on a Micromeritics 2900 TDP/TPR analyzer. Prior to analysis, each sample was heated at 873 K in an argon stream for 1 h. Measurements were made at room temperature by alternate passage of argon and the same gas containing 5% CO_2 over the sample (Fig. 1); the amount of CO_2 chemisorbed was calculated as the difference between the first adsorption peak (physisorbed plus chemisorbed amounts) and the arithmetic mean of the adsorption and desorption peaks. Basically was assessed under the assumption that one molecule of CO_2 was adsorbed on one basic site. The number of basic sites determined, n_b, was thus a measure of basicity. Basic site density, defined as the ratio of the number of basic sites to the specific surface area, can also be useful for correlation purposes since it provides a measure of the distance between adjacent basic sites.

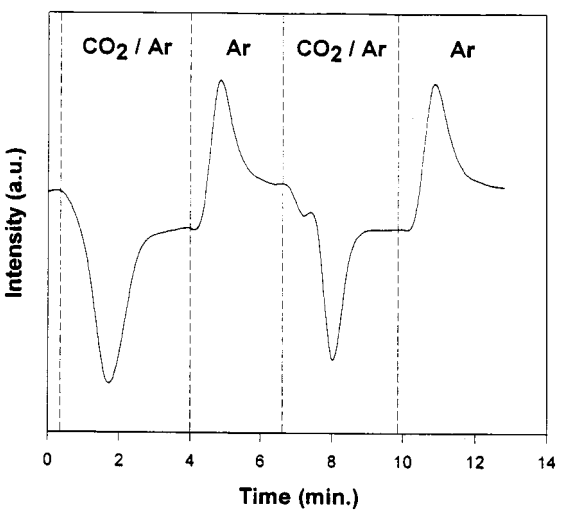

FIG. 1. CO_2 adsorption–desorption profiles for solid MgO_S.

X-ray Diffraction

X-ray diffraction patterns for the solids studied were recorded on a Siemens D-500 diffractometer using Cu$K\alpha$ radiation. Scans were performed over the 2θ range from 5 to 80°.

Solid-State Nuclear Magnetic Resonance Spectroscopy

^{1}H MAS NMR experiments were carried out at 400.13 MHz on a Bruker ACP-400 (9.4 T) spectrometer using zirconia rotors. All measurements were made at room temperature. Spectra were recorded using an excitation pulse of $\pi/2$ (5 μs) and a recycle time of 3 s. A total of 1000 free induction decays were accumulated. Chemical shifts were measured relative to an external tetramethylsilane standard. Prior to analysis by NMR spectroscopy, samples were dehydrated by evacuation in a BET apparatus at 373 K at a pressure below 3 μm of Hg overnight. Following transfer in a nitrogen atmosphere to a moisture-free nitrogen glove box, the samples were filled into the zirconia rotors, which were spun at 4 kHz during MAS NMR experiments. ^{1}H MAS NMR spectra were interpreted under the assumption that no atmospheric water penetrated the rotors into such highly hygroscopic samples. In order to justify this assumption, ^{1}H MAS NMR spectra for a sample calcined at 873 K were recorded immediately upon transfer to the rotor and several days later. Both spectra turned out to be identical to each other and rather different from those for samples exposed to moisture, so the risk of water penetrating the samples was ruled out. The ^{1}H background resonance from the probe itself, identified by recording an ^{1}H MAS NMR spectrum for an empty rotor, consisted of a broad, very low-intensity resonance—apparently a static one. All ^{1}H MAS NMR spectra used and reported in this paper were corrected for this background resonance by subtracting the "empty rotor" spectrum.

RESULTS AND DISCUSSION

Table 1 shows the specific surface areas and mean pore diameters obtained for the different solids studied. As can be seen, calcining $Mg(OH)_2$ at 873 K seemingly does not alter the specific surface area of the resulting magnesium oxide (MgO_S), which is similar to that of the commercially available oxide (MgO_C). All these solids have low specific surface areas, since the pore system consists primarily of

TABLE 1
Textural and Base Properties of the Magnesium Oxides Studied

	d_p (nm)[a]	S_{BET} ($m^2\ g^{-1}$)	n_b ($\mu mol\ CO_2\ g^{-1}$)[b]	D_b ($\mu mol\ CO_2\ m^{-2}$)[c]
$Mg(OH)_2$	20.4	14	—	—
MgO_S	24.1	15	29 ± 4	1.9 ± 0.1
MgO_{AC}	25.0	20	29 ± 1	1.4 ± 0.1
MgO_W	7.7	110	257 ± 3	2.4 ± 0.1
MgO_C	20.7	10	15 ± 1	1.5 ± 0.1

[a]Mean pore diameter.
[b]Total number of basic sites (determined by TPD measurements).
[c]Basic site density $= n_b/S_{BET}$.

macropores. Treatment with acetone altered the textural properties of the solid, the specific surface area and pores of which were slightly increased as a result. On the other hand, treatment with water dramatically increased the specific surface area, consistent with previous results (4). However, it also considerably reduced pore size, even though the pore structure of the solid continued to be compossed mainly of mesopores.

The basic properties of MgO_S and MgO_{AC} were as similar as their textural properties and also similar to those of MgO_C. Treatment with water produced a solid nearly 10 times more basic and exhibiting a much higher basic site density than the MgO_S, but lower in both cases than those obtained elsewhere by using a similar titration method (26).

Figure 2 shows the X-ray diffraction patterns for the starting, commercially available $Mg(OH)_2$, the MgO_S into which it was converted by calcination at 873 K, and MgO_C (the commercially available oxide). As can be seen, the pattern for the commercially available hydroxide (Fig. 2A) is consistent with a brucite-like $Mg(OH)_2$ phase ($2\theta = 38.1$, 18.6, 50.9, 58.7, 62.1, 68.3, 72.1, 32.9). The pattern for the solid obtained by calcining this hydroxide at 873 K (MgO_S, Fig. 2B) suggests that the solid consists of highly crystalline periclase MgO ($2\theta = 43.0$, 62.4, 78.7, 37.0, 74.8). Also, it is virtually identical to that for the commercially available magnesium oxide (Fig. 2C). In previous work, we showed the calcination of $Mg(OH)_2$ at these or higher temperatures to produce highly crystalline periclase MgO (27).

Figure 3 shows the diffraction patterns for the solids MgO_{AC} and MgO_W, in addition to the diffraction pattern for MgO_S to facilitate comparison. As can be seen, no crystal phase other than periclase MgO is produced by the water and acetone treatments. The acetone treatment (Fig. 3B) yields a periclase similarly crystalline to MgO_S; on the other hand, the water treatment (Fig. 3C) has a strong effect on crystallinity, which is considerably decreased. The relative crystallinities calculated by the Wilson–Scherrer method have shown this asumption (1.55, 1.60, and 1.96 for MgO_S, MgO_{AC}, and MgO_W, respectively).

Figure 4 shows the ^1H MAS NMR spectra for the starting $Mg(OH)_2$, its calcination product, and the commercially available magnesium oxide. As can be seen, the spectrum for the brucite $Mg(OH)_2$ (Fig. 4a) exhibits two signals centered at 1.6 and 4.5 ppm, in addition to several spinning side bands. The signal at 4.5 ppm, which is the stronger and is shifted downfield, can be ascribed to OH groups in $Mg(OH)_2$, where brucite layers are still hydroxylated. Based on the results of Brunet and Schaller (28), the signal at 1.6 ppm can be ascribed to hydroxyl groups bound to the

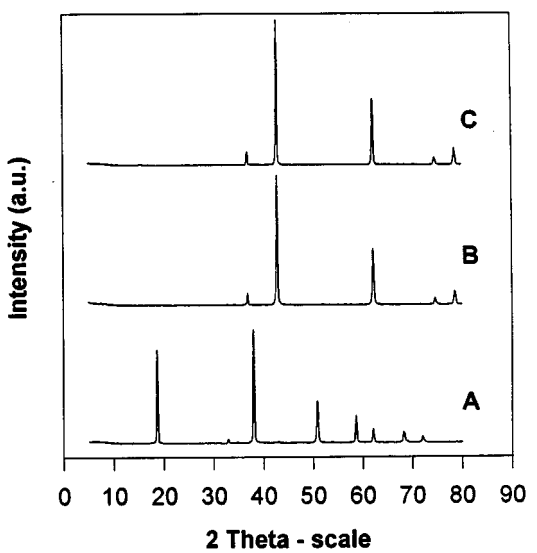

FIG. 2. XRD patterns for solids (A) $Mg(OH)_2$, (B) MgO_S, and (C) MgO_C.

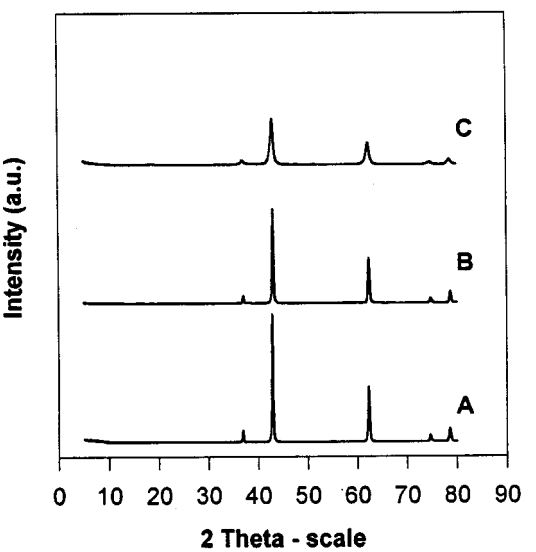

FIG. 3. XRD patterns for solids (A) MgO_S, (B) MgO_{AC}, and (C) MgO_W.

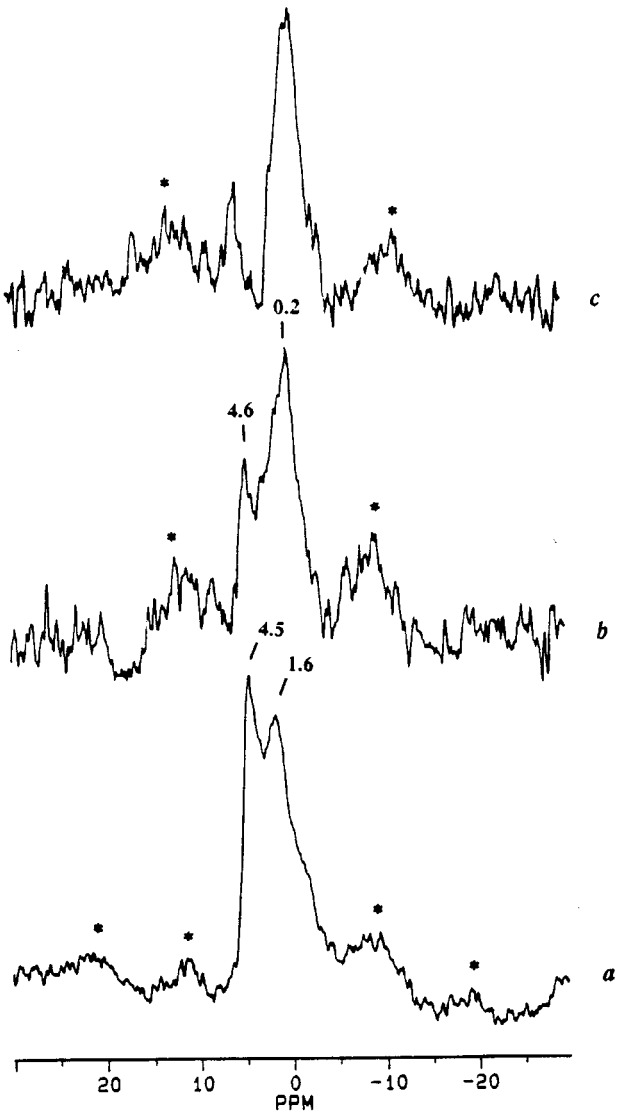

FIG. 4. ^{1}H MAS NMR spectra for solids (a) $Mg(OH)_2$, (b) MgO_S, and (c) MgO_C.

second layer of magnesium atoms. As previously inferred from the X-ray diffraction patterns, when this $Mg(OH)_2$ is calcined at 873 K it becomes periclase MgO; as can be seen in Fig. 4b, the ^{1}H MAS NMR spectrum for the periclase exhibits two major signals, at 4.6 and 0.2 ppm. The latter corresponds to "basic" OH groups, as can be inferred from their upfield shift. The signal at 4.6 ppm suggests the presence of hydrogen bonds between some OH surface groups that will obviously be of an acidic character. It should be noted that the signal at 0.2 ppm exhibits four shoulders at $-$ 1.0, 0.6, 1.1, and 1.5 ppm, which suggests a wide distribution of surface OH groups of variable basic strength. The spectrum for MgO_C (Fig. 4c) exhibits sharp signals similar to those for the previous solid; this, together with the previously determined chemical textural properties of both solids, suggests a similar distribution of surface sites.

Figures 5a and 5b show the spectra for the magnesium oxides MgO_W and MgO_{AC}, respectively. For easier comparison, the spectrum for the starting product, MgO_S, also shown in Fig. 4b, is included. One immediate conclusion is that, as shown by the above-described techniques, the acetone treatment scarcely affects the hydroxylated surface of MgO; in fact, the signal at 0.2 ppm continues to be the stonger, even though some peaks for OH groups of variable basic strength are sharper and taller than those for MgO_S, which are closer and more strongly overlapped. In contrast, treating the oxide with distilled water produces a solid, the

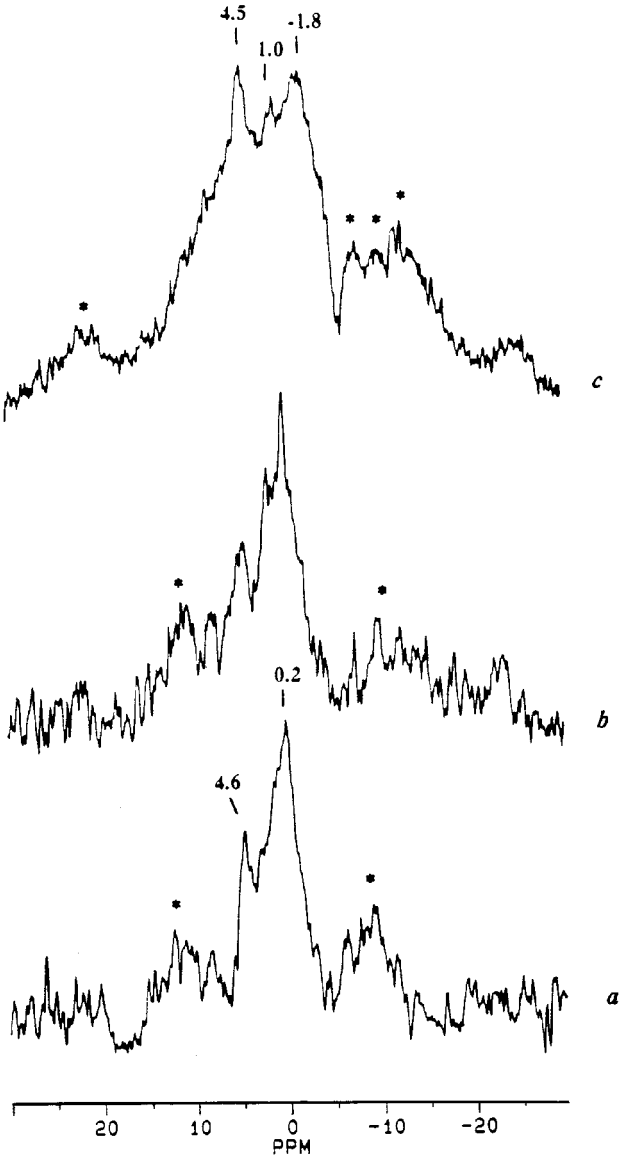

FIG. 5. ^{1}H MAS NMR spectra for solids (a) MgO_S, (b) MgO_{AC}, and (c) MgO_W.

^{1}H MAS NMR spectrum for which includes a broad signal between 10 and -4 ppm, that suggests the appearance of new hydroxyl groups strongly shifted upfield with peaks at about -1.8, 1.0, and 4.5 ppm (Fig. 5c). Therefore, rehydration increases the surface "basicity" of OH groups in this oxide relative to the previous ones, as suggested by the presence of the strongly shielded signal at -1.8 ppm, consistent with the basicity results from the CO_2 chemisorption measurements. Also, the increase in the signal at 4.5 ppm reflects an increase not in basic strength but rather in the population of acid OH groups. Finally, the signal at 1.0 ppm and the small shoulders in other signals reveal the presence of different types of OH groups with also different acid–base properties.

CONCLUSIONS

The results obtained in this work show that calcining commercially available magnesium hydroxide at 873 K produces a magnesium oxide of low surface area with a surface structure highly similar to that of commercially available magnesium oxide. No significant differences in chemical textural properties, in X-ray diffraction patterns, or in ^{1}H MAS NMR spectra appear to exist. Refluxing in acetone and subsequent calcination at 873 K results in no substantially different surface properties relative to the previous solids. On the other hand, refluxing in water and calcination at the same temperature lead to a magnesium oxide that is roughly 10 times more basic and which possesses a much higher surface area than the previous ones. This treatment yields a solid where the periclase phase is less crystalline.

ACKNOWLEDGMENTS

The authors express their gratitude to Spain's DGICyT for funding this work as a part of Project PB92-0816 and to the staff of the Nuclear Magnetic Resonance Service of the University of Córdoba for their invaluable assistance in recording the NMR spectra.

REFERENCES

1. M. A. Aramendía, V. Borau, C. Jiménez, J. M. Marinas, F. J. Romero, J. A. Navio, and J. Barrios, *J. Catal.* **157,** 97 (1995).
2. M. A. Aramendía, V. Borau, C. Jiménez, J. M. Marinas, A. Porras, and F. J. Urbano, *J. Catal.* **161,** 829 (1996).
3. M. A. Aramendía, V. Borau, C. Jiménez, J. M. Marinas, A. Porras, and F. J. Urbano, *J. Mater. Chem.* **6,** 1943 (1996).
4. T. E. Holt, A. D. Logan, S. Chakraborti, and A. K. Dayte, *Appl. Catal.* **34,** 199 (1987).
5. J. Schwank, S. Galvano, and G. J. Parravano, *J. Catal.* **63,** 415 (1980).
6. J. M. Driessen, E. K. Poels, J. P. Hinderman, and V. Ponec, *J. Catal.* **82,** 26 (1983).
7. N. K. Pande and T. Bell, *J. Catal.* **98,** 7 (1986).
8. A. K. Dayte and J. Schwank, *J. Catal.* **93,** 256 (1985).
9. Y. Doi, H. Miyake, and K. Soza, *J. Chem. Soc. Chem. Commun.* **5,** 595 (1987).
10. M. Primet, M. El Azhar, and M. Guenin, *Appl. Catal.* **50,** 241 (1990).
11. J. K. A. Clarke, M. J. Bradley, L. A. J. Garcie, A. J. Craven, and T. Baird, *J. Catal.* **143,** 122 (1993).
12. C. Doremieux-Morin, C. Martin, J. M. Bregeault, and J. Fraisard, *Appl. Catal.* **77,** 149 (1991).
13. E. C. Decanio, J. C. Edwards, and J. W. Bruno, *J. Catal.* **148,** 76 (1994).
14. V. M. Mastikhin, A. V. Nosov, V. V. Terskikh, K. I. Zamaraev, and I. E. Wachs, *J. Phys. Chem.* **98,** 13621 (1994).
15. M. Crocker, R. H. M. Herold, A. E. Wilson, M. Mackay, C. A. Emeis, and A. M. Hoogendoorn, *J. Chem. Soc. Faraday Trans.* **92,** 2791 (1996).
16. L. Jhansi-Lakshmi, S. T. Srinivas, P. Kanta-Rao, A. V. Nosov, O. B. Lapina, and V. M. Mastikhin, *Solid State NMR* **4,** 59 (1995).
17. M. A. Aramendía, V. Borau, C. Jiménez, J. M. Marinas, and J. R. Ruiz, *Solid State NMR* **8,** 251 (1997).
18. M. A. Aramendía, V. Borau, C. Jiménez, J. M. Marinas, F. J. Romero, and J. R. Ruiz, *J. Solid State Chem.* **131,** 78 (1997).
19. M. A. Aramendía, V. Borau, C. Jiménez, J. M. Marinas, F. J. Romero, and J. R. Ruiz, *J. Colloid Interface Sci.* **202,** 456 (1998).
20. M. Hunger, D. Freude, and H. Pfeifer, *J. Chem. Soc. Faraday Trans.* **87,** 657 (1991).
21. M. Hunger, S. Ernst, and J. Weitkmo, *Zeolites* **15,** 188 (1995).
22. M. Hunger, T. Horvath, G. Engelhardt, and H. G. Karge, *Stud. Surf. Sci. Catal.* **94,** 756 (1005).
23. S. Brunauer, P. H. Emmet, and E. J. Teller, *J. Am. Chem. Soc.* **60,** 73 (1951).
24. E. P. Barret, L. S. Joyner, and P. P. Halenda, *J. Am. Chem. Soc.* **73,** 373 (1964).
25. M. A. Aramendía, V. Borau, C. Jiménez, F. Lafont, J. M. Marinas, A. Porras, and F. J. Urbano, *Rapid Commun. Mass Spectrosc.* **9,** 193 (1995).
26. E. López-Salinas, M. García-Sánchez, M. E. Llanos-Serrano, and J. Navarrete-Boláñoz, *J. Phys. Chem. B.* **101,** 5112 (1997).
27. M. A. Aramendía, V. Borau, C. Jiménez, J. M. Marinas, F. J. Romero, and J. R. Ruiz, *J. Solid State Chem.* **135,** 96 (1998).
28. F. Brunet and T. Schaeller, *Am. Miner.* **81,** 385 (1996).